(3-Iminio-1-propenyl)oxy-borates: New Acyclic Betaines from Enaminocarbonyl Compounds and Boron Trifluoride or Triphenylboron – Synthesis, Crystal Structure Analysis, and Quantum Chemical Calculations

Joachim Nikolai[a], Gerhard Taubmann[b], and Gerhard Maas[a]

[a] Abteilung Organische Chemie I, Universität Ulm, Albert-Einstein-Allee 11, D-89081 Ulm, Germany
[b] Abteilung Theoretische Chemie, Universität Ulm, Albert-Einstein-Allee 11, D-89081 Ulm, Germany

Reprint requests to Prof. Dr. G. Maas. Fax: +49(731)5022803.
E-mail: gerhard.maas@chemie.uni-ulm.de

Z. Naturforsch. **58b,** 217 – 225 (2003); received October 10, 2002

Adducts of various acyclic enaminoketones and enaminoaldehydes with the Lewis acids boron trifluoride and triphenylboron were prepared. The adducts were characterized by NMR (^{1}H, ^{13}C, ^{11}B) and IR spectroscopy, FAB-MS, and X-ray crystal structure analysis of the adducts of (*E*)-3-diethylamino-3-phenyl-2-propenal with BF_3 (**4a)** and BPh_3 (**5a**), respectively. The adduct formation occurs at the oxygen atom of the enaminocarbonyl compound and gives rise to a betainic structure with expressed equalization of the bond orders in the enaminocarbonyl moiety. The gas-phase structures of complexes **4a** and **5a** and of the corresponding free enaminoaldehyde were determined computationally by RHF and DFT methods, and a Natural Bond Orbital (NBO) analysis was undertaken.

Key words: Enaminocarbonyl Compounds, Boron, Betaines, Quantum Chemical Calculations

Introduction

Lewis acid activation of carbonyl compounds is one of the important tools in synthetic organic chemistry [1]. The interaction of a Lewis acid with the carbonyl oxygen atom does not only enhance the reactivity of carbonyl compounds, *e.g.* towards nucleophilic addition to the carbonyl group and their use as dienophiles in Diels-Alder reactions [2], but it also provides stereochemical control over these and other transformations in appropriate cases [3]. Therefore, it is not surprising that chemists became interested in the nature, structure and stability of Lewis acid adducts with carbonyl compounds. In fact, a number of such adducts have been isolated and several solid-state structures have been determined. Examples with boron-based Lewis acids, which play a major role for activation of carbonyl compounds, include the benzaldehyde-BF_3 adduct **1** [4], the methacrolein-BF_3 adduct [5], and complexes of dimethyl formamide with BX_3 (X = F, Cl, Br, I) [6] and *B*-bromocatecholborane [6]. Furthermore, the solution and solid-state structures of complexes of PhC(=O)R (R = H, Me, OEt, N*i*Pr$_2$) with the highly electrophilic Lewis acid $B(C_6F_5)_3$ have been investigated recently [7].

In enaminocarbonyl compounds, the C=O bond is more polarized than in simple ketones and aldehydes, due to the contribution of a resonance structure of the type HC(=N^+R_2)—CH=CH—O^-. In line with this bond structure, enaminocarbonyl compounds are attacked by electrophiles at the oxygen atom (*e.g.* protonation, alkylation, and acylation [8], trifluoromethylsulfonylation [9]), and in particular with enaminones bearing a tertiary amino group the resulting 3-oxy-1-propene iminium salts can often be isolated. Remarkably, no simple adducts of enaminocarbonyl compounds with boron-based Lewis acids have been reported. Secondary enaminoketones react with BF_3 to form (β-imino)vinyloxyboranes **2** which maintain a six-membered cyclic structure through B—N coordination [10] (d(B—N) = 1.543(6) Å for R^1 = Ph, R^2 = R^3 = Me [10b]). Analogous compounds (R^3 = H) have been obtained from α,β-unsaturated ketones and cyanoalkyl zinc-copper reagents in a BF_3-assisted

0932–0776 / 03 / 0200–0217 $ 06.00

Michael addition / cyclization sequence and were also characterized by crystal structure analysis [11]. Products analogous to **2** are also formed from secondary enaminoketones and benzo-1,3,2-dioxaborole [12].

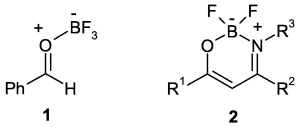

1 **2**

Here, we describe the synthesis as well as the spectroscopic and structural characterization of novel acyclic boron-based Lewis acid complexes of enaminocarbonyl compounds along with a natural bond orbital (NBO) analysis based on ab initio calculated optimized structures.

Results and Discusssion

The synthesis of 1:1 adducts **4** and **5** was achieved in a straightforward Lewis-acid/base reaction from enaminoaldehydes **3a – c** and enaminoketone **3d** with boron trifluoride etherate and triphenylboron, respectively (Scheme 1). When the Lewis acid was added to a toluene solution of **3a – d** at 45 °C, the corresponding adduct began to precipitate immediately. The remarkably stable complexes **4** and **5** could be washed with diethyl ether or even acetonitrile without decomposition. However, addition of excess DMSO-d_6 to **5d** at 20 °C resulted in the formation of enaminoketone **3d** and the complex $(CD_3)_2S{=}O \rightarrow BPh_3$ ($\delta(^{11}B) = 7.2$).

The bonding in the complexes **4** and **5** can be described by the mesomeric structures **A** and **B** shown in Scheme 2, where **B** emphasizes the delocalization of positive charge into the enaminone's conjugated system. Several NMR arguments are in agreement with the betainic iminium-borate structure **B** of the novel complexes. In the ^{13}C NMR spectra, carbon atom C-1 is shielded with respect to the carbonyl signal of enaminones **3**, while the N-substituted atom C-3 is deshielded (Table 1). These changes are larger in the cases of BF_3 adducts **4a**,**b**, in agreement with the higher Lewis acidity of BF_3 vs. BPh_3. In the ^1H NMR spectra, the aldehyde proton suffers a high-field shift, and the olefinic proton 2-H a low-field shift on complexation (δ = 7.1 – 7.6 and 5.5 – 6.1 ppm, respectively). A *trans* configuration at the C1—C2 bond can be expected for steric reasons and was confirmed by a crystal structure analysis (*vide infra*); in the ^1H NMR spectra, this geometry is characterized by ^3J(1-H, 2-H) coupling constants around 10 Hz. The observation of separate signals for the two NCH_2 groups in each adduct (except for **5b** where these signals are just coalescing) indicates hindered rotation around the C—N bond and is in line with the presence of an iminium ($C{=}N^+$) group, but it is not *per se* typical of the adducts because separate signals are also seen in the free enaminones. However, a comparison of **3a** (two broad, unstructered signals, beginning coalescence) and adducts **4a**,**5a** (two sharp quartets) under identical conditions (400 MHz, ca. 30 °C) indicates the higher double bond (*i.e.* enhanced $C{=}N^+$) character in the adducts.

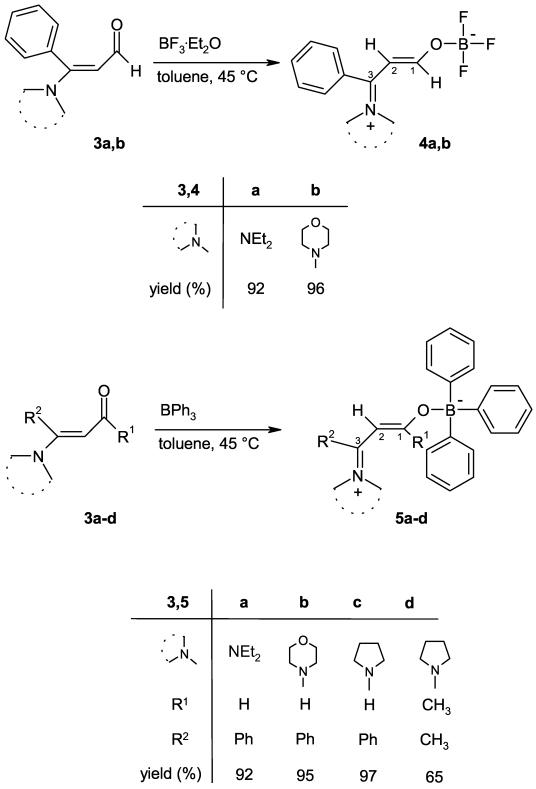

3,4	a	b
	NEt_2	
yield (%)	92	96

3,5	a	b	c	d
	NEt_2			
R^1	H	H	H	CH_3
R^2	Ph	Ph	Ph	CH_3
yield (%)	92	95	97	65

Scheme 1. Preparation of Lewis acid adducts of enaminocarbonyl compounds.

The ^{11}B signals of the BF_3 adducts **4a**,**b** are found at $\delta = -0.4$ and -0.3 ppm, respectively, those of the BPh_3 adducts at $\delta = 8.4 - 8.8$ (**5a – c**) and 9.7 ppm (**5d**). These values are quite close to those reported for BF_3 complexes with carbonyl compounds in general and for the BPh_3-dimethyl formamide complex, respectively (note that enaminoaldehydes are vinylogous formamides) [13]. Thus, only a minor change is observed when the ether ligand of $BF_3{\cdot}Et_2O$

Table 1. Complexation induced changes of ^{13}C chemical shifts (δ, ppm); $\Delta\delta$ is the difference between the free enaminones **3a–d** and the corresponding complex **4** or **5**.

Complex	**4a**	**4b**	**5a**	**5b**	**5c**	**5d**
δ(CO), complex	181.1	182.9	187.8	188.4	185.7	191.5
δ(CO), free	190.5	191.7	190.5	191.7	189.0	193.6
$\Delta\delta$(CO)	−9.4	−8.8	−2.7	−3.3	−3.3	−2.1
$\delta(C_{sp2}N)$, complex	176.1	176.4	174.0	171.4	169.8	165.4
$\delta(C_{sp2}N)$, free	166.7	167.8	166.7	167.8	164.5	159.3
$\Delta\delta(C_{sp2}N)$	+7.6	+8.6	+7.3	+3.6	+5.3	+6.1

Table 2. Selected bond lengths (Å) and angles (°) in the solid state structures of **4a** (at 193 K) and **5a** (at 293 K).

	4a[a]	**5a**
Bond lengths and angles:		
B—O	1.496(3), 1.496(3)	1.597(2)
O—C1	1.307(2), 1.302(2)	1.286(2)
C1—C2	1.357(2), 1.357(3)	1.362(2)
C2—C3	1.422(3), 1.416(3)	1.405(2)
C3—N	1.315(2), 1.325(2)	1.320(2)
B—F	1.370(3) — 1.382(3), 1.370(3) — 1.377(3)	—
B—O—C1	118.7(2), 120.3(2)	117.1(1)
O—C1—C2	122.2(2), 122.4(2)	125.1(2)
Torsion angles:		
F1—B—O—C1	178.5(2), 169.9(2)	177.8(1)
B—O—C1—C2	171.9(2), −174.6(2)	178.2(2)
O—C1—C2—C3	179.8(2), −179.6(2)	-177.9(2)
C1—C2—C3—N	176.3(2), -176.2(2)	-175.5(2)
C2—C3—C8—C9	93.3(2), -99.3(3)	74.5(2)
Intermolecular contacts[b] *H···F (Å), C—H···F (°)*:		
C2—H2···F1*^{I}	2.45, 170.0	
C13—H13···F2^{II}	2.43, 134.5	
C6*—H6*b···F1^{I}	2.49, 142.1	
C9*—H9*···F2*^{III}	2.41, 159.6	

[a] Two independent molecules in the unit cell. [b] Starred atoms refer to the second independent molecule; symmetry operations: $0.5-x$, $-0.5+y$, $-0.5-z$; II: $-x$, $1-y$, $-z$; III: $1.5-x$, $-0.5+y$, $0.5-z$.

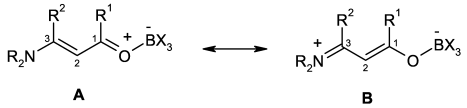

Scheme 2. Resonance structures of enaminocarbonyl-borane complexes.

($\delta(^{11}B)$ = 0.0) is replaced by enaminoaldehydes. On the other hand, the resonance of free BPh_3 (δ = 68.0 [13]) suffers an appreciable upfield shift on complexation with either formamides or enaminocarbonyl compounds.

In the IR spectra, enaminocarbonyl compounds **3** are characterized by two strong absorptions in the ranges 1614 – 1634 and 1533 – 1543 cm^{-1}. In the complexes **4** and **5**, these absorptions are replaced by bands

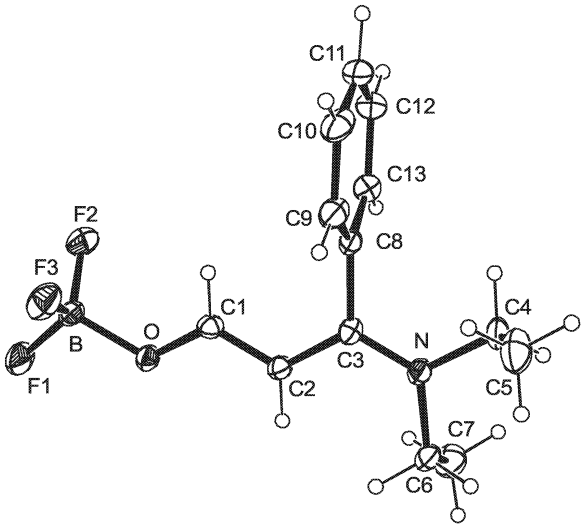

Fig. 1. Molecular structure of **4a** in the crystal; the ellipsoids of thermal vibration represent a 30% probability. Only one of the two symmetry-independent molecules is shown.

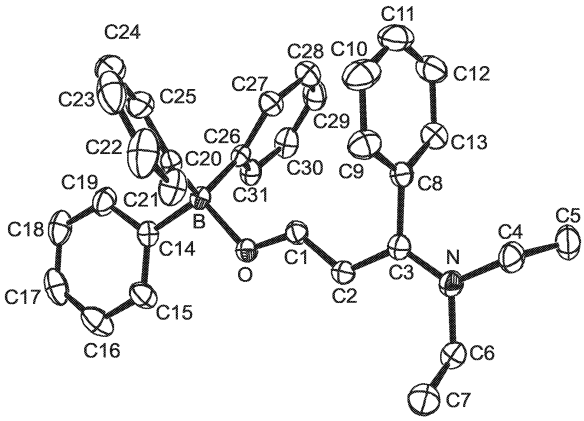

Fig. 2. Molecular structure of **5a** in the crystal; the ellipsoids of thermal vibration represent a 30% probability.

at 1585 – 1609 and 1548 – 1576 cm^{-1}. In both, the enaminones [8a] and the complexes, these absorptions are attributed to the whole of the conjugated system rather than localized vibrations of C=C, C=O and/or C=N^{+} bonds.

FAB mass spectra, showing basis peaks for the [MH^{+}-BF_3] ion, indicate that the oxygen-boron bond is the least strong bond in complexes **4a**,**b**. Fragmentation at the O—B bond was also observed for **5a – c**, but the loss of a phenyl group from [M^{+}] gives rise to the basis peak in compounds **5a – d**.

The solid state structures of **4a** and **5a** were determined by X-ray crystal structure analysis. ORTEP

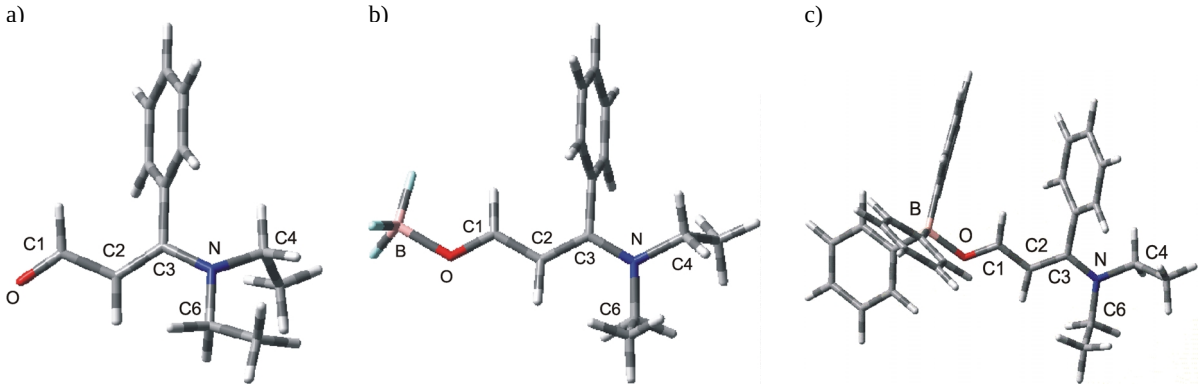

Fig. 3. B3LYP/6-31G* optimized structures of a) **3a**, b) **4a**, c) **5a**.

plots [14] of the complexes are shown in Figures 1 and 2. Complex **4a** crystallizes with two independent molecules in the unit cell. Selected values of the bond geometry are given in Table 2.

The results confirm the O-coordination of the Lewis acid in both cases, and they reveal an almost planar zigzag configuration of the B—O—C_3—N chain. With the phenyl ring at C3 approximately orthogonal to the plane defined by these atoms, this arrangement is clearly expected on steric grounds. This geometry includes an anti coordination of the Lewis acid at the carbonyl group and the *E* configuration at the C1—C2 bond. The bond distances in the enaminocarbonyl moiety of the two structures show similar deviations from values of unbiased systems: The C3—N bond is longer than a localized C=N^+ bond (*e.g.*, 1.265(6) Å in a propyne iminium salt [15]) but shorter than a C—N_{sp2} bond in enamines (1.355(14) Å [16]). The C1—C2 distance, representing a C_{sp^2}—C_{sp^2} single bond in the free enaminoaldehyde, has become shorter than the C2—C3 bond and is not much elongated with respect to an unperturbed double bond (1.32(1) Å [16]). The C1—O distance is longer than a C=O double bond found in aldehydes (1.192(5) Å) but shorter than a C—O bond in enols and enol derivatives (1.33 – 1.35 Å [16]). The bond length values indicate that through the O-complexation with a Lewis acid, the enaminoaldehyde moiety of betaines **4a** and **5a** experiences an expressed equalization of bond orders.

The B—O distances (1.496 Å in **4a**, 1.592 Å in **5a**) are in the upper range of known oxygen-boron bond lengths (1.38 – 1.61 Å [16]). The significantly shorter B—O bond length in **4a** correlates with a somewhat longer C1—O bond length than in **5a**, both changes indicating the stronger coordination of the harder Lewis acid BF_3. The B—O bond length in **4a** is also shorter than in the benzaldehyde-BF_3 complex [4] (1.496 *vs.* 1.591 Å). On the other hand, the B—O bond in **5a** is longer by 0.07 Å than in the adduct PhC(O)N*i*Pr_2-$B(C_6F_5)_3$ [8]. A tighter contact in the latter complex may be caused not only by the higher electrophilicity of that borane but also by the presence of π-stacking between the phenyl group of the benzamide and one phenyl ring of BAr_3 [8], a feature not seen in the solid-state structure of **5a**.

The two independent molecules in the unit cell of **4a** show some significant differences in torsion angles (Table 2). Pairs of them are in a quasi-centrosymmetric spatial relationship in which their phenyl rings intersect at an angle of 7.2° and maintain C_{ipso}—C_{ipso} distances of 3.51 Å and one C_{meta}—C_{meta} distance of 3.61 Å. Several weak C—H···F interactions are found in the crystal structure with values (2.41 – 2.49 Å, Table 2) that are shorter than the sum of the van der Waals radii of hydrogen and fluorine (2.67 Å [17]).

We were interested to learn whether the experimentally obtained bonding features in complexes **4a** and **5a** could also be reproduced with reasonable agreement by methods of computational chemistry. Therefore, we perfomed restricted Hartree-Fock (RHF) and density functional theory (DFT) calculations of these complexes using Gaussian 98 [18]. In order to elaborate the influence of the complexation with BF_3 or BPh_3 on the structure of enaminoaldehyde **3a**, this compound was treated at the same level of theory. The results are summarized in Table 3. Figure 3 shows the DFT optimized structures of **3a**, **4a**, and **5a**.

Both the RHF and B3LYP optimized structures show the expected changes of bond geometries between free **3a** and complexes **4a** and **5a**: changes of

Table 3. Selected bond lengths (Å) and angles (°) for RHF and DFT optimized structures of **3a**, **4a**, and **5a**; see Figs. 1 and 2 for atom numbering.

Compound	**3a**				**4a**				**5a**	
Level of theory	RHF /6-31G*	RHF /6-31+G*	B3LYP /6-31G*	B3LYP /6-31+G*	RHF /6-31G*	RHF /6-31+G*	B3LYP /6-31G*	B3LYP /6-31+G*	RHF /6-31G*	B3LYP /6-31G*
B—O	—	—	—	—	1.599(7)	1.563(3)	1.618(3)	1.591(4)	1.637(8)	1.623(6)
O—C1	1.197(0)	1.199(7)	1.225(8)	1.230(5)	1.239(4)	1.244(5)	1.260(0)	1.268(8)	1.236(5)	1.265(7)
C1—C2	1.464(4)	1.462(3)	1.454(2)	1.450(6)	1.406(2)	1.400(6)	1.400(0)	1.404(3)	1.409(3)	1.407(2)
C2—C3	1.346(3)	1.350(1)	1.372(0)	1.375(9)	1.379(9)	1.386(8)	1.390(0)	1.396(9)	1.378(8)	1.394(0)
C3—N	1.387(8)	1.383(8)	1.388(4)	1.384(4)	1.336(2)	1.332(1)	1.350(0)	1.351(2)	1.340(9)	1.356(7)
C3—N—C6	117.5(9)	117.6(8)	118.1(8)	118.3(7)	121.2(9)	121.3(7)	121.2(4)	121.4(1)	120.8(2)	120.9(0)
C3—N—C4	117.8(4)	118.3(4)	119.2(4)	119.8(0)	123.9(4)	123.9(6)	123.3(9)	123.4(5)	123.3(2)	123.0(7)
C4—N—C6	116.4(1)	116.5(2)	116.4(0)	116.6(5)	114.7(3)	114.6(2)	115.0(3)	114.9(7)	115.1(5)	115.3(6)
E_{total}	−631.468[a]	−631.484[a]	−635.574[a]	−635.599[a]	−954.697[a]	−954.726[a]	−960.164[a]	−960.216[a]	−1346.554[a]	−1355.415[a]
ZPE[b]	0.295[a]	0.294[a]	0.275[a]	−0.275[a]	0.311[a]	0.309[a]	0.291[a]	0.289[a]	0.593[a]	0.555[a]
NImag[c]	0	0	0	0	0	0	0	0	0	0

[a] Hartree per molecule; [b] *ZPE*: zero point energy; [c] *Nimag*: number of imaginary frequencies.

Table 4. Wiberg bond indices for **3a**, **4a**, and **5a**.

Compound	**3a**		**4a**		**5a**	
level of theory[a]	RHF	B3LYP	RHF	B3LYP	RHF	B3LYP
B—O	–	–	0.41	0.44	0.49	0.53
O—C1	1.72	1.74	1.37	1.43	1.35	1.40
C1—C2	1.11	1.15	1.29	1.32	1.30	1.33
C2—C3	1.66	1.59	1.45	1.44	1.45	1.43
C3—N	1.11	1.16	1.27	1.29	1.26	1.29

[a] RHF and B3LYP stand for RHF/6-31G* and B3LYP/6-31G*, respectively. In all cases, results from single point calculations based on B3LYP/6-31G* optimized structures are given.

bond lengths in the enaminone backbone towards the iminium enolate structure (**B**, Scheme 2) and planarization at the enamine nitrogen atom. The values obtained with the DFT method are in general closer to the experimentally determined values. However, at both levels of theory, the C1—O and C2—C3 bonds are shorter and the C1—C2 and C3—N bonds are longer with respect to the values obtained by X-ray diffraction. In the calculated structures, the C1—C2 and C2—C3 bond lengths in **4a** and **5a** are almost the same at the DFT level, but the experimentally found bond length reversal at these two bonds, with respect to free **3a**, is not reproduced. This is also illustrated by the Wiberg bond indices [19] (Table 4).

The DFT-calculated B—O and C1—O bond lengths are virtually the same in the two complexes. Those for **5a** agree within 0.021 – 0.025 Å with the experimentally found value. The same is not true for BF_3 complex **4a** for which the calculated B—O distance is almost the same as in the BPh_3 complex but longer by 0.12 Å than the experimental value, while the calculated C1—O distance is shorter by 0.04 Å. Thus, the calculations do not seem to distinguish between enaminoaldehyde complexation by BF_3 vs. BPh_3, in contrast to the tighter complexation of BF_3 as suggested by the crystal structure analysis of **4a**. According to the Wiberg bond indices (Table 4), the bond order of the B—O bond should even be a little higher in **5a** than in **4a**, in distinct contrast to the experimental values. For comparison, we calculated the B—O bond length for the adducts methacrolein-BF_3 and benzaldehyde-BF_3 which have been characterized by X-ray analysis [4,5]. On the B3LYP/6-31+G* level of theory, we found a B—O bond length of 1.69 Å for methacrolein-BF_3 [X-ray: 1.58 Å] and 1.67 Å for benzaldehyde-BF_3 [X-ray: 1.49 Å]. Again, the calculated bond lengths are longer by 0.11 and 0.18 Å than the experimental values. From these systematic deviations in the B—O bond lengths of the calculated structures, and with all other geometrical parameters in quite good agreement, we conclude that the generally observed shortening of the B—O bond length in crystal structures of BF_3 adducts as compared to the calculated structures is due to packing effects such as the presence of intermolecular (B)F···H—C hydrogen bonds (*vide supra*). Computational investigations of this aspect are in progress and will be reported in due course.

Charges found by natural population analysis [20,21] (Table 5) give an alternating charge distribution for the free enaminoaldehyde as expected on the basis of Lewis resonance formulas. This charge distribution is conserved in **4a** and **5a**. In contrast to the negative formal charge on the boron atom and the positive formal charge on the nitrogen atom suggested by the Lewis formula for **4a** and **5a**, a positive charge on the boron atom and a negative charge on the nitrogen atom is found in the natural population analysis. This appar-

Table 5. Natural population analysis for **3a**, **4a**, and **5a**.

Compound	**3a**		**4a**		**5a**	
Level of theory[a]	RHF	B3LYP	RHF	B3LYP	RHF	B3LYP
B	–	–	1.581	1.381	0.808	0.341
O	−0.660	−0.563	−0.725	−0.594	−0.677	−0.469
C1	0.480	0.343	0.529	0.362	0.539	0.225
C2	−0.480	−0.419	−0.543	−0.437	−0.537	−0.278
C3	0.331	0.236	0.441	0.305	0.442	0.332
N	−0.551	−0.445	−0.506	−0.391	−0.512	−0.417

[a] RHF and B3LYP stand for RHF/6-31G* and B3LYP/6-31G*, respectively. In all cases, results of single point calculations based on B3LYP/6-31G* optimized structures are given.

ent discrepancy is associated with the fact that Lewis formulae are simply drawn following the octet rule, whereas in the quantum chemical calculations differences in electronegativity of the individual atoms are included.

In conclusion, we have reported the first acyclic complexes of enaminoaldehydes and enaminoketones with boron-based Lewis acids. The complexation occurs through carbonyl coordination and changes the bond structure of the free enaminocarbonyl compound towards an iminium enolate structure. Since the nitrogen lone pair is engaged in this bonding, intramolecular B—N coordination, in addition to B—O coordination, cannot take place.

Computational Methods

Hartree-Fock (RHF) and density functional theory (DFT, B3LYP functional) methods using Gaussian type basis sets implemented in the Gaussian 98 program package were used for geometry optimizations [18]. Standard convergence criteria as implemented in the modelling program without using any geometry constraints were applied. All calculated structures reported are minima on the potential energy surface (only positive eigenvalues of the Hessian matrix). For **5a**, optimizations were perfomed with the 6-31G* basis set only, since addition of diffuse functions made the calculations too large to be perfomed within acceptable time.

Population analysis and Wiberg bond indices were calculated with the program package NBO 3.1 [20] implemented in Gaussian 98. Since NBO 3.1 cannot handle linearly dependent basis sets generated by RHF/– and DFT/6-31+G* calculations, Wiberg bond index calculations and population analyses were perfomed with the 6-31G* basis set. All calculations were done on 900 MHz UltraSPARCIII+ Solaris 9 computers at the Universitätsrechenzentrum Ulm.

Experimental Section

All reactions were carried out in rigorously dried glassware under an Ar atmosphere. Et_2O was distilled from Na and stored under argon. CH_2Cl_2 was dried over P_2O_5, distilled and stored under argon. NMR spectra were recorded at 303 K on Bruker DRX 400 and Bruker Avance 400 spectrometers (^{1}H: 400.13 MHz; ^{13}C: 100.61 MHz; ^{19}F: 376.47 MHz) and on a Bruker AMX 500 instrument (^{11}B: 160.46 MHz). TMS served as internal standard for ^{1}H and $CDCl_3$ (δ = 77.0 ppm) or CD_2Cl_2 (δ = 53.5 ppm) for ^{13}C NMR spectra. All ^{13}C NMR spectra were recorded proton-decoupled; assignments of ^{13}C chemical shifts are based on DEPT 135 spectra. For the ^{19}F NMR spectra, $CFCl_3$ was used as an external standard. For the ^{11}B NMR spectra, triethylborate ($B(OEt)_3$, 15% *v*/*v* in $CDCl_3$) was used as external capillary standard (δ = 18.1 ppm) [22]. IR spectra were measured on a Bruker Vector 22 spectrophotometer. Positive mode FAB mass spectra were performed on a Finnigan TSQ 7000 instrument. Melting points were determined with an apparatus after Dr. Tottoli (Büchi) (heating rate 2 °C/min) and are uncorrected. Bulb-to-bulb distillations were carried out in a Büchi GKR 50 apparatus, the temperatures given refer to the heating mantle. Microanalyses were performed with a Perkin-Elmer Analyser 2400 CHN.

Starting materials: Enaminoketone **3d** [23] and triphenylboron [24] were prepared according to literature procedures. Boron trifluoride etherate was purchased from Fluka. Enaminoaldehydes **3a**,**b** were prepared as published [25]. Detailed spectroscopic data for these compounds are given here, since they have not yet been reported.

(E)-3-Diethylamino-3-phenyl-propenal (**3a**)*:* Preparation from phenylpropynal and diethylamine according to lit. [25]; yellow oil, b.p. 185 °C/ 0.02 mbar (Kugelrohr) (lit. [25]: 142 – 144 °C/0.01 Torr). The oil solidifies on standing, m.p. 70 °C. – IR (film): ν = 1614 (s), 1536 (vs), 1260 (s), 1204 (s), 795 (s), 775 (s), 731 (s), 701 (s) cm^{-1}. – ^{1}H NMR ($CDCl_3$): δ = 0.94, 1.19 (very br, each 3 H, CH_3), 2.93, 3.34 (very br, each 2 H, CH_2), 5.34 (d, J = 8.5, 1 H, =CH), 7.19 (m, 2 H_{Ph}), 7.35 (m, 3 H_{Ph}), 8.48 (d, J = 8.5, 1 H, CHO); the *E* configuration was assigned by a NOESY experiment. – ^{13}C NMR ($CDCl_3$): δ = 11.3, 14.2 (both br, CH_3), 42.3, 45.1 (both br, NCH_2), 102.2 (C-2), 127.2, 128.2, 128.8, 133.8 (C_{Ph}), 166.7 (C-3), 190.5 (CHO).

(E)-3-Morpholino-3-phenylpropenal (**3b**)*:* Preparation from phenylpropynal and morpholine according to lit. [25]; orange powder, m.p. 106 °C (lit. [25]: 112 °C). – IR (KBr): ν = 1623 (s), 1542 (s), 1394 (s), 1188 (s), 790 (s), 739 (s), 702 (s) cm^{-1}. – ^{1}H NMR ($CDCl_3$): δ = 3.21 (br, 4 H, OCH_2CH_2N), 3.71 (br, 4 H, OCH_2CH_2N), 5.47 (d, J = 8.3, 1 H, =CH), 7.30 (m, 2 H_{Ph}), 7.45 (m, 3 H_{Ph}), 8.81 (d, J = 8.3, 1 H, CHO); the *E* configuration was assigned by a NOESY experiment. – ^{13}C NMR ($CDCl_3$): δ = 47.9 (br,

OCH_2CH_2N), 66.3 (br, OCH_2CH_2N), 104.7 (C-2), 128.6, 129.5, 129.8, 133.4 (C_{Ph}), 167.8 (C-3), 191.7 (CHO).

(E and Z)-3-Pyrrolidino-3-phenyl-propenal (**3c**)*:* The solution of pyrrolidine (0.64 ml, 7.7 mmol) and phenylpropynal (1.00 g, 7.7 mmol) in EtOH (15 ml) was refluxed for 5 h. After removal of the solvent, bulb-to-bulb distillation of the brown oily residue at 190 °C/10^{-3} mbar afforded 1.30 g (82%) of an orange oil which solidified on standing, m.p. 112 °C. According to the ^{1}H NMR spectrum, a mixture of *E* and *Z* diastereomers (78:22) was obtained. – IR (film): ν = 1634 (s), 1580 (s), 798 (m), 753 (m) cm^{-1}. – ^{1}H NMR ($CDCl_3$): *E*-**3c**: δ = 1.79 (t, *J* = 7.0, 2 H, CH_2), 1.98 (t, *J* = 7.0, 2 H, CH_2), 2.98 (t, *J* = 7.0, 2 H, NCH_2), 3.31 (t, *J* = 7.0, 2 H, NCH_2), 5.25 (d, *J* = 8.7, 1 H, ═CH), 7.20 (m, 2 H_{Ph}), 7.36 (m, 3 H_{Ph}), 8.63 (d, *J* = 8.7, 1 H, CHO); *Z*-**3c**: δ = 1.96, 1.98 (both br, 2 H, CH_2), 3.21, 3.48 (br, 2 H, NCH_2), 5.61 (d, *J* = 12.3, 1 H, ═CH), 7.20 and 7.36 (3 $H_{m,p-Ph}$), 7.81 (d, *J* = 6.4, 2 H_{o-Ph}), 7.94 (d, *J* = 12.3, 1 H, CHO). – ^{13}C NMR ($CDCl_3$): *E*-**3c**: δ = 24.0, 24.2 (NCH_2CH_2), 47.4, 49.1 (NCH_2), 102.5 (C-2), 126.5-128.2, 133.7 (C_{Ph}), 164.5 (C-3), 189.0 (CHO); *Z*-**3c**: δ = 129.7 (C_{Ph}), 139.6 (C_{Ph}), 184.0 (CHO), other signals hidden by major isomer or not found. – $C_{13}H_{15}NO$ (201.3): calcd. C 77.58, H 7.51, N 6.96; found C 77.48, H 7.49, N 6.88.

(3-Dimethyliminio-3-phenyl-(E)-prop-1-enyl)oxy-trifluoroborate (**4a**)*:* To a solution of **3a** (0.44 g, 2.2 mmol) in toluene (5 ml), kept at 45 °C, $BF_3{\cdot}Et_2O$ (0.30 ml, 2.4 mmol) was added in one portion. An oil separated which turned into a slight yellow precipitate upon vigorous stirring of the mixture. The toluene layer was discarded, and the crude product was washed with Et_2O to afford 0.54 g (92%) of a colorless powder, m.p. 155 °C. – IR (KBr): ν = 1607 (s), 1570 (s), 1313 (s), 1263 (s), 1119 (s), 1080 (s), 947 (s), 947 cm^{-1}. – ^{1}H NMR (CD_2Cl_2): δ = 1.11 (t, *J* = 7.2, 3 H, CH_3), 1.39 (t, *J* = 7.2, 3 H, CH_3), 3.24 (q, *J* = 7.2, 2 H, CH_2), 3.67 (q, *J* = 7.2, 2 H, CH_2), 6.05 (d, *J* = 10.1, 1 H, 2-H), 7.24 (d, *J* = 6.6, 2 H_{o-Ph}), 7.41 (d, *J* = 10.1, 1 H, 1-H), 7.52-7.55 (m, 3 $H_{m,p-Ph}$). – ^{13}C NMR (CD_2Cl_2): δ = 12.0, 13.6 (both CH_3), 46.2, 48.8 (both CH_2), 102.7 (C-2), 127.9, 129.3, 130.8, 131.1 (C_{Ph}), 176.1 (C═N^+), 181.1 (C-1). – ^{19}F NMR (CD_2Cl_2): δ = −154.7. – ^{11}B NMR (CD_2Cl_2): δ = −0.4. – MS (+FAB, m-NBA): *m/z* (%) = 252 (20) [M^+-F], 204 (100) [MH^+-BF_3], 186 (20) [MH^+-BF_3, -H_2O]. – $C_{13}H_{17}BF_3NO$ (271.08): calcd. C 57.60, H 6.32, N 5.17; found C 57.16, H 6.31, N 5.01.

[3-(1-Azonia-4-oxacyclohexylidene)-3-phenyl-(E)-prop-1-enyl]oxy-trifluoroborate (**4b**)*:* To a solution of **3b** (0.39 g, 1.8 mmol) in toluene (5 ml), kept at 45 °C, $BF_3{\cdot}Et_2O$ (0.25 ml, 1.9 mmol) was added in one portion. An oily layer formed which was separated from the toluene layer and was diluted with a little dichloromethane. Diethyl ether was added to precipitate a light-pink solid which was washed with Et_2O to leave 0.49 g (96%) of **4b**, m.p. 160 °C (dec.). – IR (KBr): ν = 1609 (s), 1576 (m), 1341 (s), 1248 (s), 1118 (s), 1083 (m), 943, 905 (s, br) cm^{-1}. – ^{1}H NMR (CD_2Cl_2): δ = 3.50 (pseudo-t, 2 H, OCH_2CH_2N), 3.63 (pseudo-t, 2 H, OCH_2CH_2N), 3.82-3.89 (m, 4 H, OCH_2CH_2N), 6.10 (d, *J* = 10.5, 2-H), 7.27 (d, *J* = 6.8, 2 H_{o-Ph}), 7.51-7.59 (m, 4 H, 1-H, $H_{m,p-Ph}$). – ^{13}C NMR (CD_2Cl_2): δ = 50.0, 52.0 (OCH_2CH_2N), 66.1, 66.9 (OCH_2CH_2N), 102.6 (C-2), 128.6, 128.6, 129.6, 130.3, 131.9 (C_{Ph}), 176.4 (C═N^+), 182.9 (C-1). – ^{19}F NMR (CD_2Cl_2): δ = −154.4. – ^{11}B NMR (CD_2Cl_2): δ = −0.3. – MS (+FAB, m-NBA): *m/z* (%) = 266 (75) [M^+-F], 218 (100) [MH^+-BF_3], 200 (26) [MH^+-BF_3, -H_2O]. – $C_{13}H_{15}BF_3NO$ (285.07): calcd. C 54.77, H 5.30, N 4.91; found C 54.13, H 5.38, N 4.72.

(3-Diethyliminio-3-phenyl-(E)-prop-1-enyl)oxy-triphenylborate (**5a**)*:* To a solution of BPh_3 (0.89 g, 3.7 mmol) in toluene (8 ml) was added at 45 °C in one portion aldehyde **3a** (0.75 g, 3.7 mmol) dissolved in toluene (8 ml). The precipitate formed immediately after the complete addition of the aldehyde was allowed to settle. After removal of the solvent, the residue was washed twice with Et_2O to yield 1.5 g (92%) of a beige powder, m.p. 170 °C (dec.). – IR (KBr): ν = 1586 (s), 1547 (s), 1337 (s), 1258 (s), 1160 (m), 702 (s) cm^{-1}. – ^{1}H NMR ($CDCl_3$): δ = 1.07 (t, *J* = 7.1, 3 H, CH_3), 1.36 (t, *J* = 7.1, 3 H, CH_3), 3.13 (q, *J* = 7.1, 2 H, CH_2), 3.53 (q, *J* = 7.1, 2 H, CH_2), 5.97 (d, *J* = 9.9, 1 H, 2-H), 6.98-7.39 (m, 20 H_{Ph}), 7.52 (d, *J* = 9.9, 1 H, 1-H). – ^{13}C NMR ($CDCl_3$): δ = 12.2, 14.2 (CH_3), 45.5, 47.9 (CH_2), 101.4 (C-2), 124.8, 127.0, 128.2, 129.0, 130.5, 131.8, 133.6, 154.7 (C_{Ph}), 174.0 (C═N^+), 187.8 (C-1). – ^{11}B NMR ($CDCl_3$): δ = 8.8. – MS (+FAB, m-NBA/DMF): *m/z* (%) = 444 (43) [M^+-H], 368 (100) [M^+-Ph], 204 (26) [MH^+-BPh_3]. – $C_{31}H_{32}BNO$ (445.4): calcd. C 83.52, H 7.18, N 3.14; found C 83.53, H 7.19, N 3.07.

[3-(1-Azonia-4-oxacyclohexylidene)-3-phenyl-(E)-prop-1-enyl]oxy-triphenylborate (**5b**)*:* Synthesis as described for **5a**, from BPh_3 (0.21 g, 0.9 mmol) in toluene (2 ml) and **3b** (0.18 g, 0.9 mmol) in toluene (2 ml). Yield: 0.38 g (95%), beige powder, m.p. 187 °C. – IR (KBr): ν = 1585 (s), 1548 (s), 1348 (s), 1328 (s), 1244 (s), 1116 (m), 708 (m) cm^{-1}. – ^{1}H NMR (CD_2Cl_2): δ = 3.1-3.8 (two very broad signals, coalescing, 8 H, OCH_2CH_2N), 5.97 (d, *J* = 9.8, 2-H), 6.97-7.14 (m, 16 H_{Ph}), 7.25-7.29 (m, 2 H_{Ph}), 7.36-7.40 (m, 2 H_{Ph}), 7.67 (d, *J* = 9.8, 1 H, 1-H). – ^{13}C NMR (CD_2Cl_2): δ = 48.2, 48.7 (OCH_2CH_2N), 65.5 (OCH_2CH_2N), 101.4 (C-2), 123.8, 125.9, 128.1, 129.7, 130.9, 132.5, 134.1, 153.2 (C_{Ph}), 171.4 (C═N^+), 188.4 (C-1). – ^{11}B NMR (CD_2Cl_2): δ = 8.5. – MS (+FAB, m-NBA): *m/z* (%) = 459 (3) [M^+], 382 (100) [M^+-Ph], 218 (93) [MH^+-BPh_3]. – $C_{31}H_{30}BNO_2$ (459.4): calcd. C 81.05, H 6.58, N 3.05; found C 80.83, H 6.49, N 2.92.

[3-(1-Azoniacyclopentylidene)-3-phenyl-(E)-prop-1-enyl]oxy-triphenylborate (**5c**)*:* Synthesis as described for **5a**, from BPh_3 (0.26 g, 1.1 mmol) in toluene (3 ml) and **3c** (0.22 g, 1.1 mmol) in toluene (4 ml). Yield: 0.46 g (97%),

Table 6. Crystal data and details of structure refinement for **4a** and **5a**.

	4a	**5a**
Empirical formula	$C_{13}H_{17}BF_3NO$	$C_{31}H_{32}BNO$
Formula weight	271.09	445.39
Crystal dimensions, [mm]	$0.31 \times 0.23 \times 0.15$	$0.46 \times 0.31 \times 0.19$
Temp, K	193(2)	293(2)
Crystal system	monoclinic	monoclinic
Space group	$P2_1/n$ (no. 14)	$P2_1/n$ (no. 14)
a, [Å]	15.824(4)	13.435(3)
b, [Å]	10.436(2)	13.750(2)
c, [Å]	17.572(4)	14.038(2)
α, [deg]	90	90
β, [deg]	105.04(3)	90.92(2)
γ, [deg]	90	90
Z; D_{calc} [g cm^{-3}]	8, 1.285	4, 1.141
Θ Range [min/max]	2.01/24.10	2.07/24.10
μ(Mo-K_α) [cm^{-1}]	0.107	0.067
Data collected, unique	17606, 4371	16207, 4048
Completeness to Θ_{max}, [%]	98.2	98.4
R_{int}	0.0737	0.0388
No. of obsd. data ($I > 2\sigma(I)$)	2294	2409
No. of refined parameters	347	309
$R1$ (obs./ all data)[a]	0.0353/0.0887	0.0374/0.0723
$wR2$ (obs./ all data)[a]	0.0606/0.0689	0.0854/00996
Max/min residual electron density, e Å^{-3}	0.21/−0.13	0.11/−0.14

[a] $R = \Sigma(||F_o| - |F_c||)/\Sigma|F_o|$; $wR2 = [\Sigma[w(F_o^2 - F_c^2)^2]/\Sigma[(wF_o^2)^2]]^{1/2}$.

beige powder, m.p. 186 °C (dec.). – IR (KBr): ν = 1588 (s), 1551 (s), 1353 (s), 1322 (s), 1233 (s), 702 (s) cm^{-1}. – ^{1}H NMR ($CDCl_3$): δ = 1.70 (m, 2 H, CH_2), 1.90 (m, 2 H, CH_2), 3.03 (t, J = 6.9, NCH_2), 3.29 (t, J = 6.9, NCH_2), 5.73 (d, J = 10.2, 2-H), 6.86 (d, J = 7.1, 2 H_{o-Ph}), 6.94-6.98 (m, 3 H_{Ph}), 7.03-7.06 (m, 6 H_{Ph}), 7.17-7.21 (m, 8 H_{Ph}), 7.25-7.28 (m, 1 H_{Ph}), 7.52 (d, J = 10.2, 1 H, 1-H). – ^{13}C NMR ($CDCl_3$): δ = 23.7, 24.0 (CH_2), 48.7, 50.9 (NCH_2), 100.8 (C-2), 123.5, 125.6, 126.6, 127.7, 129.2, 131.1, 132.6, 153.1 (C_{Ph}), 169.8 (C═N^+), 185.7 (C-1). – ^{11}B NMR ($CDCl_3$): δ = 8.4. – MS (+FAB, m-NBA/DMSO): *m/z* (%) = 442 (2) [M^+-H], 366 (100) [M^+-Ph], 202 (41) [MH^+-BPh_3]. – $C_{31}H_{30}BNO$ (443.4): calcd. C 83.97, H 6.82, N 3.16; found C 82.87, H 6.86, N 3.16.

[4-(1-Azoniacyclopentylidene)-but-2-enyl]oxy-triphenylborate (**5d**)*:* Synthesis from BPh_3 (0.50 g, 2.1 mmol) in toluene (6 ml) and **3d** (0.32 g, 2.1 mmol) in toluene (10 ml). Yield: 0.53 g (65%), beige powder. An analytically pure sample was obtained by vapor diffusion of Et_2O into a saturated solution of **5d** in CH_2Cl_2 at 20 °C; m. p. 183 °C (dec.). – IR (KBr): ν = 1566 (s), 1534 (s), 1477 (s), 1331 (s), 72 (s), 730 (s) cm^{-1}. – ^{1}H NMR (CD_2Cl_2): δ = 1.81 (br, 3 H, CH_3), 1.94 (br, 4 H, CH_2), 2.62 (s, 3 H, CH_3), 3.31 (br, 2 H, NCH_2), 3.47 (br, 2 H, NCH_2), 5.03 (s, 2-H), 7.02-7.06 (m, 3 H_{Ph}), 7.13-7.16 (m, 6 H_{Ph}), 7.38-7.40 (m, 6 H_{Ph}). – ^{13}C NMR (CD_2Cl_2): δ = 19.0 (CH_3), 24.0, 24.1 (CH_2), 27.7 (CH_3), 48.7, 48.9 (NCH_2), 96.5 (C-2), 123.6, 125.8, 132.6, 154.2 (C_{Ph}), 165.4 (C═N^+), 191.5 (C-1). – ^{11}B NMR (CD_2Cl_2): δ = 9.7. – MS (+FAB, m-NBA/DMSO): *m/z* (%) = 394 (5) [M^+-H], 380 (6) [M^+-CH_3], 318 (100) [M^+-Ph]. – $C_{27}H_{30}BNO$ (395.3): calcd. C 82.03, H 7.65, N 3.54; found C 81.98, H 7.53, N 3.54.

X-ray diffraction analysis of betaines (**4a**) *and* (**5a**)

Crystals of **4a** and **5a** suitable for X-ray diffraction analysis were obtained by vapor diffusion of Et_2O into a saturated solution of **4a** (**5a**) in CH_2Cl_2 at 20 °C. Data collection on single crystals was performed with an imaging-plate diffractometer (IPDS, Stoe) using monochromatized Mo-K_α radiation (λ = 0.71073 Å). The structures were solved with direct methods and refined with full-matrix least-squares procedures using F^2 values [26]. Hydrogen atoms are in calculated positions and were treated by the riding model. Relevant crystal data and details of the structure determination are given in Table 5. Crystallographic data have been deposited as CCDC-191845 (for **4a**) and -191846 (for **5a**). These data can be obtained free of charge via www.ccdc.cam.ac.uk/conts/retrieving.html (or from the Cambridge Crystallographic Data Centre, 12, Union Road, Cambridge CB2 1EZ, UK; fax: (+44)1223-336-033).

Acknowledgements

The help of Prof. Dr. H.-U. Siehl, Dr. G. Schmidtberg and Dr. U. Werz (all at Ulm), and Prof. Dr. C. G. Kreiter (^{11}B NMR, University of Kaiserslautern) is gratefully acknowledged. J. N. thanks the Land Baden-Württemberg for a post-graduate fellowship. The calculations were made possible in the frame of the Center of Excellence for Computational Chemistry, a collaborative project between the University of Ulm and Sun Microsystems (http://www.uni-ulm.de/coe).

[1] a) S. Shambayati, S. L. Schreiber, in B. M. Trost, I. Fleming (eds.): Comprehensive Organic Synthesis, Vol. 1, chapter 1.10, Pergamon Press, Oxford (1991); b) H. Yamamoto (ed.), Lewis Acid Reagents – A Practical Approach, Oxford University Press, New York (1999).

[2] a) W. Oppolzer, Angew. Chem. **96**, 840 – 864 (1984); Angew. Chem. Int. Ed. **23**, 876 – 889 (1984); b) F. Fringuelli, A. Taticchi, The Diels-Alder Reaction – Selected Practical Methods, John Wiley & Sons, Chichester (2002).

[3] E. J. Corey, Angew. Chem. **114**, 1724 – 1741 (2002); Angew. Chem. Int. Ed. **41**, 1650 – 1667 (2002).
[4] M. T. Reetz, M. Hüllmann, W. Massa, S. Berger, P. Rademacher, P. Heymanns, J. Am. Chem. Soc. **108**, 2405 – 2408 (1986).
[5] E. J. Corey, T.-P. Loh, S. Sarshar, M. Azimiora, Tetrahedron Lett. **33**, 6945 – 6948 (1992).
[6] E. J. Corey J. J. Rohde, A. Fischer, M. D. Azimioara, Tetrahedron Lett. **38**, 33 – 36 (1997).
[7] D. J. Parks, W. E. Piers, M. Parvez, R. Atencio, M. J. Zaworotko, Organometallics **17**, 1369 – 1377 (1998).
[8] a) J. V. Greenhill, Chem. Soc. Rev. **6**, 277 – 294 (1977); b) H. E. A. Kramer, R. Gompper, Z. Phys. Chem. (Frankfurt am Main) **43**, 349 – 370 (1964); c) O- vs. C2-protonation: H. Böhme, M. Tränka, Liebigs Ann. Chem. 149 – 159 (1985).
[9] B. Singer, G. Maas, Chem. Ber. **120**, 485 – 495 (1987).
[10] a) K. Itoh, K. Okazaki, A. Sera, Y. L. Chow, J. Chem. Soc., Chem. Commun. 1608 – 1609 (1992); b) K. Itoh, M. Fujimoto, M. Hashimoto, Acta Crystallogr. C**54**, 1324 – 1327 (1998).
[11] M. C. P. Yeh, P. Knochel, W. M. Butler, S. C. Berk, Tetrahedron Lett. **51**, 6693 – 6696 (1988).
[12] Y. P. Singh, P. Rupani, A. Singh, A. K. Rai, R. C. Mehrota, R. D. Rogers, J. L. Atwood, Inorg. Chem. **25**, 3076 – 3081 (1986).
[13] H. Nöth, B. Wrackmeyer, Nuclear Magnetic Resonance Spectroscopy of Boron Compounds, in P. Diehl, E. Fluck, R. Kosfeld (eds.): NMR, Basic Principles and Progress, Vol. 14, Springer-Verlag, Berlin (1978).
[14] L. J. Farrugia, ORTEP-3 for Windows, Version 1.062, J. Appl. Crystallogr. **30**, 565 (1997).
[15] G. Maas, R. Rahm, D. Mayer, W. Baumann, Organometallics **14**, 1061 – 1066 (1995), and references cited therein.
[16] F. H. Allen, O. Kennard, D. G. Watson, L. Brammer, A. G. Orpen, R. Taylor, J. Chem. Soc. Perkin Trans II, S1 – S19 (1987).
[17] A. Bondi, J. Phys. Chem. **68**, 441 – 451 (1964).
[18] a) Gaussian 98, Revision A.11, M. J. Frisch, G. W. Trucks, H. B. Schlegel, G. E. Scuseria, M. A. Robb, J. R. Cheeseman, V. G. Zakrzewski, J. A. Montgomery (Jr.), R. E. Stratmann, J. C. Burant, S. Dapprich, J. M. Millam, A. D. Daniels, K. N. Kudin, M. C. Strain, O. Farkas, J. Tomasi, V. Barone, M. Cossi, R. Cammi, B. Mennucci, C. Pomelli, C. Adamo, S. Clifford, J. Ochterski, G. A. Petersson, P. Y. Ayala, Q. Cui, K. Morokuma, P. Salvador, J. J. Dannenberg, D. K. Malick, A. D. Rabuck, K. Raghavachari, J. B. Foresman, J. Cioslowski, J. V. Ortiz, A. G. Baboul, B. B. Stefanov, G. Liu, A. Liashenko, P. Piskorz, I. Komaromi, R. Gomperts, R. L. Martin, D. J. Fox, T. Keith, M. A. Al-Laham, C. Y. Peng, A. Nanayakkara, M. Challacombe, P. M. W. Gill, B. Johnson, W. Chen, M. W. Wong, J. L. Andres, C. Gonzalez, M. Head-Gordon, E. S. Replogle, and J. A. Pople, Gaussian, Inc., Pittsburgh PA, 2001; b) J. B. Foresman, A. Frisch, Exploring Chemistry with Electronic Structure Methods, Gaussian Inc, Pittsburgh (1993).
[19] K. Wiberg, Tetrahedron **24**, 1083 – 1096 (1968).
[20] Gaussian NBO Version 3.1, E. D. Glendening, A. E. Reed, J. E. Carpenter, F. Weinhold.
[21] A. E. Reed, R. B. Weinstock, F. Weinhold, J. Chem. Phys. **83**, 735 – 746 (1985).
[22] J. D. Kennedy, in J. Mason (ed.): Multinuclear NMR, Plenum Press, New York (1987), pp 221 – 253, and references cited therein.
[23] G. Opitz, E. Tempel, Liebigs Ann. Chem. **699**, 69 – 73 (1966).
[24] G. Wittig, P. Raff, Liebigs Ann. Chem. **573**, 195 – 209 (1951).
[25] F. Wille, F. Knörr, Chem. Ber. **85**, 851 – 992 (1952).
[26] G. M. Sheldrick, SHELX-97 – Program for the solution and refinement of crystal structures from diffraction data, University of Göttingen, Germany (1997).